APCC
APEC CLIMATE CENTER

TECHNICAL REPORT

APCC
APEC CLIMATE CENTER

PREFACE

It is our pleasure to present to you the APEC Climate Center (APCC)'s Technical Report 2012, which reports the core outcomes of our research activities from the past year.

Since 2005, APCC, as a hub of climate information in the Asia-Pacific region, has strived to share our analysis and prediction of abnormal climate and to apply this information to regional development. The Center has established the most extensive Multi-Model Ensemble (MME) system for seasonal prediction in the world through its international science network and has provided value-added products to various stakeholders. Recently, APCC has expanded its mandate to include enhancing the capacity of APEC member economies to respond effectively to climate change and variability through better application of climate information.

In 2012, APCC continued to make an effort to improve the quality and quantity of our short-term climate forecasts and our online climate information systems, as information dissemination tools. Additionally, APCC began its endeavor to produce more applicable climate information through interdisciplinary research among various sectors, such as agriculture and hydrology. The following technical report provides more information about our research outcomes from 2012.

In 2013, following APCC's goal to enhance socioeconomic well-being through better utilization of climate information, APCC will continue to improve the quality and accuracy of its climate information, recognizing that the utility of this information is only as good as its quality. We would like to make the best use of our research outcomes in various scientific and application areas. We welcome any feedback on this report or on our services.

My best and warmest regards to all of you.

Dr. Chin-Seung Chung
Director/APEC Climate Center

CONTENTS

Study of Aerosol Effect on Accelerated Snow Melting over the Tibetan Plateau Using Satellite and CMIP5 Simulation Data

■■ Dr. Woo-Seop Lee

APCC

TECHNICAL REPORT 2012-02

Study of Aerosol Effect on Accelerated Snow Melting over the Tibetan Plateau Using Satellite and CMIP5 Simulation Data

Dr. Woo-Seop Lee

ABSTRACT

The warming of the atmosphere related to the absorption of aerosols has an influence on snow cover, which thereby reduces the effect of reflectance after deposition. The warming produces an atmospheric dynamical feedback, termed an "elevated-heat-pump (EHP) effect", which increases moisture, cloud cover, and deep convection over northern India, as well as enhancing the rate of snow melt in the Himalayas and on the Tibetan Plateau (TP). Observations and models were analyzed to explore the impact of these processes on the spring-time climate.

Observational evidence is firstly presented, illustrating that the Indo-Gangetic Plain (IGP) region, which is bounded by the high-altitude Himalayan mountains, is subject to heavy loading of absorbing aerosols, i.e., black carbon and dust. This leads to widespread enhancement warming over the Tibetan Plateau and accelerated snowmelt on the western Tibetan Plateau (WTP) and the Himalayas. In terms of the aerosol loading over the IGP, the two pre-monsoon seasons of 2004 and 2005 were strikingly contrasting. In 2004, the warming of the TP was widespread relative to 2005. It covered most of the WTP and the Himalayas and was closely linked to the patterns of snow melt. Consistent with the Elevated Heat Pump hypothesis, we find that an increased loading of absorbing aerosols over the IGP in the pre-monsoon season is associated with an increased heating of the upper troposphere, which enhances the rate of snowmelt over the Himalayas and the WTP in April-May.

Secondly, a coupled atmosphere-ocean global climate model (CSIRO-Mk3.6) is used to investigate the role of aerosol forcing agents as drivers of snow melting trends in the TP region. Our results suggest that the heating trend of the atmosphere by aerosols can lead to widespread enhanced warming over the TP and to snow melt in the western TP and Himalayas. An aerosol layer, composed mainly of dust transported from adjacent deserts and black carbon from local emissions, builds up in the Boreal Spring over the Indo-Gangetic Plain against the foothills of the Himalayas and the TP. This layer, which extends from the surface to a high elevation, heats the mid-troposphere by absorbing solar radiation. The heating then produces an acceleration of the rate of snow melt in the Himalayas and on the TP.

PART I : Satellite observations of enhanced pre-monsoon aerosol loading and tropospheric warming over Tibetan Plateau

1. INTRODUCTION

Atmospheric aerosols are of great importance to the global climate because of their absorbing as well as scattering properties, which, in turn, significantly influence the Earth's radiation budget (Ramanathan *et al.*, 2001; Haywood and Boucher, 2000; Bellouin *et al.*, 2005). In theory, aerosols could offset greenhouse warming by directly scattering sunlight back into space and by indirectly enhancing cloud albedo, thereby cooling the climate. However, because they absorb solar radiation, absorbing aerosols heat the atmosphere, which in turn increases greenhouse warming (Jacobson, 2001). Absorbing aerosols such as black carbon and dust are thought to affect the hydrology and radiative forcing over Asia (Ramanathan and Carmichael, 2008; Menon *et al.*, 2002; Lau and Kim., 2007; Lee and Kim., 2010) as well as cause an increase in snow melt in snow covered regions (Jacobson, 2004; Flanner *et al.*, 2007; Koch *et al.*, 2009; Lau *et al.*, 2010; Lee and Kim., 2011).

The Tibetan Plateau (TP) is located close to regions in South and East Asia that have been, and are predicted to continue to be, the largest source of black soot in the world (Bond *et al.*, 2007; Ohara *et al.*, 2007). Extensive amounts of black carbon and dust aerosols are lifted to the high TP and incorporated in snowflakes. When these snowflakes subsequently fall onto glaciers, there is a visible darkening of the surface, which has led to initial studies of the amount of black carbon (BC) in the snow and ice of the Himalayan glaciers (Flanner *et al.*, 2007). Etienne *et al.* (2007) showed that 915km^2 of Himalayan glaciers thinned by an annual average of 0.85 cm between 1994 and 2004.

A recent model study by Lau *et al.* (2010) showed that the heating of the troposphere by elevated dust and black carbon aerosols in the boreal spring can lead to widespread enhanced warming of the land-atmosphere, and accelerated snow

melt in the Himalayas and western TP region. The snow cover of the Tibetan Plateau and Himalayas is very important for the regional climatic processes and hydrological cycle. In recent years, there has been growing evidence of increased warming, accompanied by early snow melt and the retreat of high mountain glaciers in the Himalayas and the TP regions (IPCC, 2007; He *et al.*, 2003; Jain, 2008; Ren *et al.*, 2006; Kulkarni et al 2007).

Until now, most studies of snow melt in the Himalayas and TP have focused on greenhouse warming (Duan *et al.*, 2006, Oerlemans 2005, Kulkarni *et al.*, 2002, Jiawen 2006). However, the rate of greenhouse warming is of the order of 0.1–0.15°C per decade, whilst the warming of the TP has been estimated to be much faster, at 0.32°C per decade (Liu and Chen, 2000), and was estimated to be at a rate of 0.7–1.2°C per decade from 1977–1994 over the Himalayan foothill regions and Middle Mountain regions in Nepal (Shresth at el., 1999). Based on the differences in the rates of warming, it is not difficult to surmise that global warming is not the sole agent of change in these regions, and that local forcing and feedback processes are likely to play an important role in causing the faster warming rate and accelerated retreat of the mountain glaciers. There are many factors which, in addition to greenhouse warming, could lead to an accelerated warming over the Himalayas and TP, such as increased land-use and land change, increased sunlight duration from a reduction in cloud cover, increased water vapor feedback, and the reduction of snow albedo caused by deposition of soot and dust on the snow surface (Kang *et al.*, 2000, Prasad and Singh 2007, Flanner *et al.*, 2007, 2009, Yasunari *et al.*, 2009). Ramanathan *et al.*, (2007) recently estimated that atmospheric heating by Asian Brown Clouds (ABC) doubles greenhouse warming over South Asia, and may contribute substantially to the loss of glacier mass in the Himalayas. Lau and Kim (2006) and Lau *et al.* (2006) proposed the so-called “Elevated-Heat-Pump (EHP)” effect, whereby heating of the atmosphere by elevated absorbing aerosols strengthens the local atmospheric circulation, leading to a northward shift of the monsoon rainfall belt. However, the effect of absorbing aerosol related reduction of snow cover/albedo and its contribution to snow/ice retreat have only begun to receive attention. There

is, therefore, need for more extensive observation data, such as data obtained from satellite observation. In this article, we present observational relationships between aerosol and snow/ice melt over the Himalayas and the Tibetan Plateau, which seem to be consistent with the EHP effect. We also present the basic features of the EHP hypothesis, and how the effect of the EHP may cause an enhanced heating in the mid-troposphere and lead to an accelerated melting of snow. Using CMIP5 model simulation, we investigate the impact of atmospheric heating by aerosols in the boreal spring, which could lead to an enhanced pre-summer monsoon surface warming and early snow melt in the Himalayas and the TP region. Our analysis focuses on the changes in the spring time snowpack over the TP and the subsequent impact on surface radiative flux changes and the hydrological cycle.

2. Data and Methodology

Moderate Resolution Imaging Spectroradiometer (MODIS) is a 36-channel visible-to-thermal-infrared sensor that was launched as part of the EOS Terra payload on December 18, 1999. Various snow and ice products are produced with MODIS imagery and the data are available at a variety of spatial and temporal resolution (Hall *et al.*, 2001). The quality of MODIS snow data has been evaluated (e.g., Pu *et al.*, 2007) and results indicate that the overall accuracy is about 90% over the TP region. In this study, a preliminary version of the gridded global monthly snow cover product MOD10CM is used, at a 0.05° resolution covering March 2000 to 2009. The most challenging task in the compiling of monthly files was the correct handling of missing values in the daily product, MOD10 Level 2, from which the monthly values are derived.

The aerosol optical depth has been obtained using Level-3 MODIS gridded atmosphere monthly global product 'MOD08_M3'(ESDT Long Name: MODIS/Terra Aerosol Cloud Water Vapor Ozone Monthly L3 Global 1Deg CMG). The monthly average

MOD08_M3 product files are produced at a spatial resolution of 1 degree by 1 degree. The elevation data used in this study were obtained from the USGS GTOPO30 Digital Elevation Model (DEM) data set (http://edc.usgs.gov/products/elevation/gtopo30/gtopo30.html). The resolution of elevation data in GTOPO30 is 30-arc seconds (approximately 1 km at the equator). We re-sampled the 30-arc seconds GTOPO30 data to 0.05° CMG grid by the area average in accordance with the resolution of MODIS SCFs.

The Atmospheric Infrared Sounder (AIRS) is on board NASA's Earth observing system satellite Aqua (EOS-Aqua). The geophysical parameters have been averaged and binned into 1°x1° grid cells, from -180.0° to +180.0° longitude and from -90.0° to +90.0° latitude. AIRS provides several atmospheric parameters, including vertical profiles of atmospheric temperature. The accuracy of temperature and water vapor profiles is expected to be 1 K for 1 km levels and 15% for 2 km layers in the troposphere, respectively (Tobin *et al.*, 2006). In this study we use the AIRS Level 3 Monthly Gridded Retrieval Product.

For wind, temperature and moisture, we used the reanalysis data from Modern Era Retrospective-analysis for Research and Applications (MERRA) (Kim *et al.*, 2006). This study uses a standard monthly mean output that is provided on 42 pressure levels at a horizontal resolution of 1.25° latitude × 1.25° longitude for the period 2000–2009.

3. Results

3.1 Aerosol Optical Depth over IGP

Figure 1 shows the large aerosol loading over the latitude-time section (70–90E) of the IGP region during the boreal spring. The aerosol optical thickness ("AOT") is abundant beginning in late winter, and peaks in May and June (to about two times the mean winter value) and then rapidly decreases in July and August following

the onset of the monsoon rains. A secondary peak is seen in November to December. The largest accumulation begins in April, peaks in May, and diminishes in July through August, due to being washed-out by monsoon rainfall (Lee and Kim 2010;). In this study we focus only on the build-up phase during April and May (AM) over the Tibetan Plateau region ("TP").

Figure 2.(a) shows the terrain elevation of the Himalayan and Tibetan Plateau. The TP is the highest and largest plateau in the world. It covers an area of 3.6 million km^2 at 2000 m above mean sea level (Qian *et al.*, 2011). The valley-type topography of the IGP is bounded by the elevated Himalayan Mountains to its north.

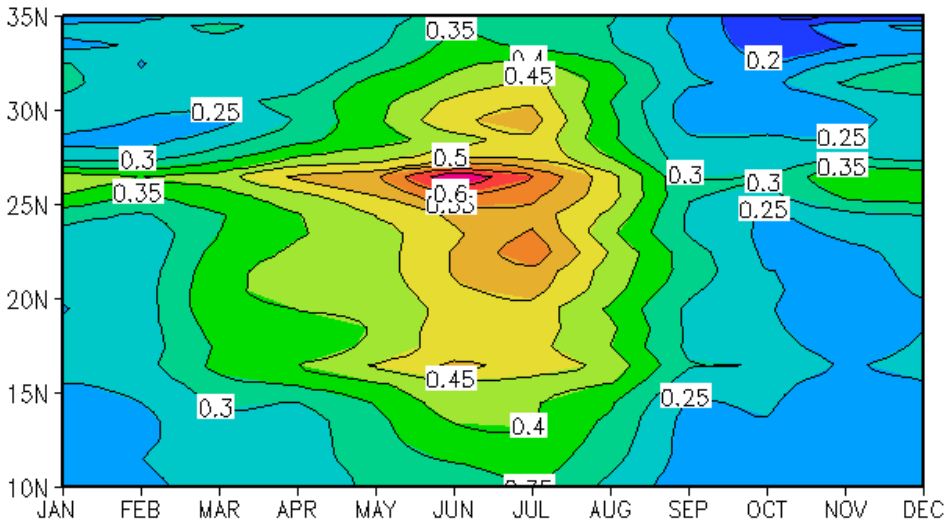

Figure 1 Latitude monthly distribution of aerosol optical thickness (AOT) over the longitudinal band 70–90°E.

The fundamental characteristics of absorbing aerosols over the Indian Subcontinent are summarized in Figure 2. Figure 2.(b) shows the AM climatological (2000–2009) distribution of aerosols from MODIS Aerosol Optical Depth ("AOD") over the Asian region. The pre-monsoon AM aerosols are clearly piled up against the Himalayan foothills, and have a distinct maximum over the IGP with a northwestward extension towards Pakistan. Climatologically, the lower-tropospheric

subsidence over northwestern India associated with the westerly flow across Afghanistan and Pakistan plays a major role in building up the aerosol layer during spring (Dey *et al.*, 2004).

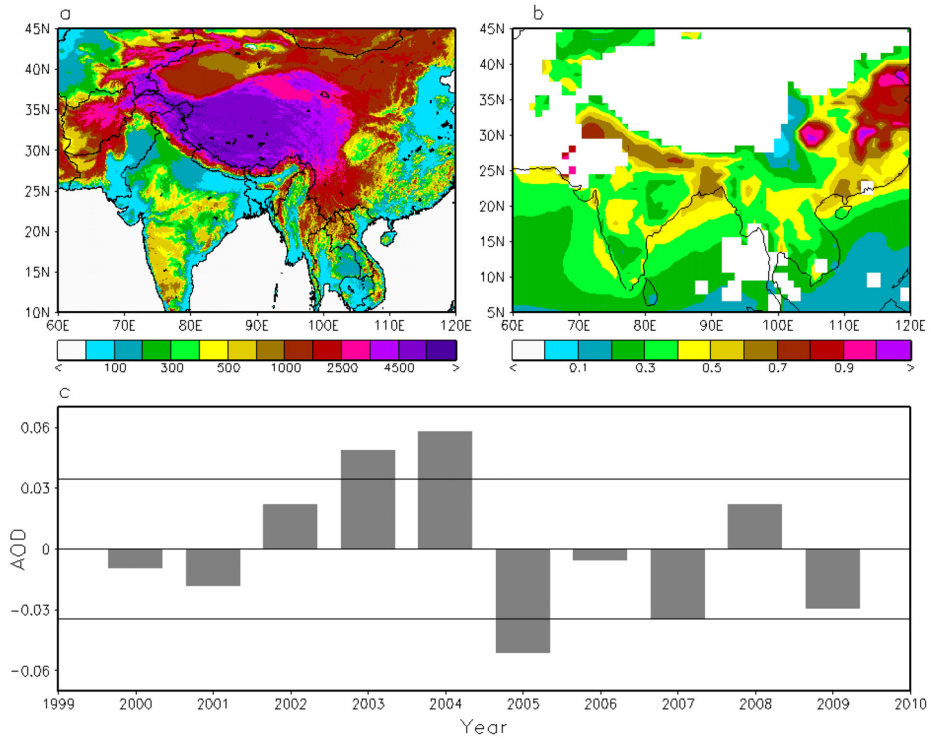

Figure 2 (a) Terrain of the Asian region; and (b) Mean MODIS AOD during pre-monsoon season (April-May)(AM) from 2000 to 2009; and (c) Inter-annual variations of AOD over IGP (20–30N, 70–90E) during April-May(AM). Straight lines indicate the standard deviation.

During the pre-monsoon season, in AM, aerosols produced by industrial activities and biomass and biofuel burning, together with those of transported dust, rapidly build up over the IGP and East Asia (Figure 2.(b)). The highest (AOD > 0.8) is found over central and northeastern China. Over Southern Asia, the aerosol level is high (AOD > 0.4) in the IGP, and around the slopes of the TP, as evident by the 0.3 AOD contour outlining the topographic contour of the TP. Figure 1.(c) shows inter-annual variations of the mean AOD in AM over the IGP region from 2000 to 2009. It can be seen that the 2004(2005) AOD is significantly higher (lower) over

the IGP compared to individual years. A significant difference in the magnitude of the aerosol loading over the IGP is discernible between the pre-monsoon seasons (AM) of 2004 and 2005. Although the patterns of aerosol loading are similar during the two periods, the entire IGP is characterized by an enhanced aerosol loading in AM 2004 compared with AM 2005. It is evident that the AODs over the IGP are 0.52 and 0.41 during the pre-monsoon periods of 2004 and 2005, respectively. It was also found that the 2004 Nino3 index (0.29) was very similar to the 2005 Nino3 index (0.26).

We therefore focused on the two pre-monsoon seasons of 2004 and 2005 that are found to be strikingly contrasting in terms of the contribution from absorbing aerosols in the atmospheric regional aerosol loading.

3.2. Enhanced warming over the TP

There is a cooling of the surface temperature difference between 2004 and 2005 near the surface of Central India Plateau (Figure 3a) due to aerosol forcing. This is due to the dimming effect, i.e., an atmospheric scattering and absorption of solar radiation, reducing the amount reaching the earth's surface. In contrast to the surface cooling in the land region of India, a pronounced surface warming appears over and around the TP ($\Delta T > 3$), especially over the Himalayan and western TP, where the climatological snow cover is more extensive compared to the TP interior. The warming extends over large regions, covering northwestern Asia, (including Kazakhstan and Pakistan), and northeastern China, (including Mongolia).

The increase of the tropospheric meridional temperature gradient associated with the consistent cooling over South Asia, together with warming over the elevated heat source of the Tibetan Plateau region during AM, produces lower sea level pressure (SLP) anomalies over Northern India relative to those over Southern India and a corresponding anomalous southwesterly over India which carries moisture from the Indian Ocean to the Indian land area. It also brings warmer air from the lower troposphere, up and over the TP (Figures 3,(c),(d)).

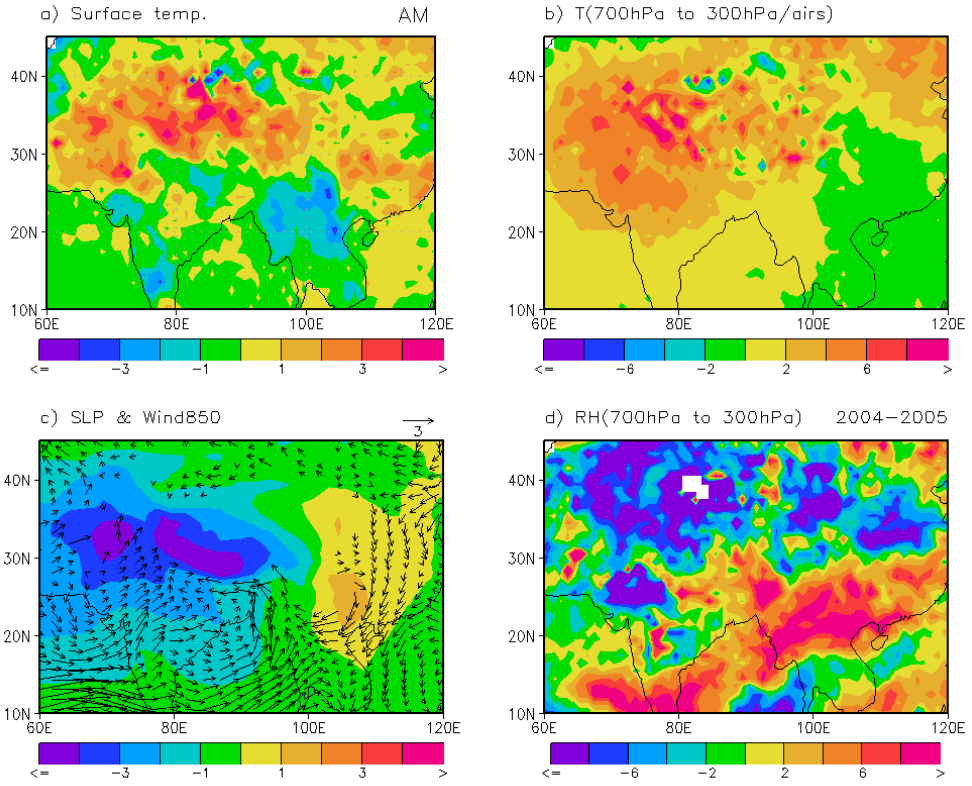

Figure 3 Maps showing the difference between April-May(AM) 2004 and April-May(AM) 2005 (2004 minus 2005) in: (a) surface temperature[°C]; (b) layer mean temperature between 700 hPa and 300 hPa[°C]; (c) sea level pressure (hPa) and 850 hPa wind; and (d) layer mean relative humidity between 700 hPa and 300 hPa (%).

Associated with the pre-monsoon surface warming over the TP is a large-scale warming in the middle to upper troposphere (Figure 3.(b)) completely covering South Asia, and an increased relative humidity over the southern part of India and the foothills of the Himalayas. However, the absorbing aerosol loading is small in regions where there is surface warming, and has a much larger spatial scale than the aerosol distribution, as shown in Figure 1.(a). These warming patterns cannot therefore be explained solely by the aerosol effect, as it is evident that the warming is dynamically induced by a circulation change associated with the EHP mechanism, rather than by the aerosol effect. The EHP has been described in previous studies (Lau *et al.*,

2006; Lau and Kim, 2006) and is briefly described below in the context of the warming and snow melt of the western TP and Himalayas.

Dust aerosols are transported from deserts (Pakistan/Afghanistan, Middle East, Sahara, and Taklamakan) adjacent to the Asian monsoon region, and accumulate at a high elevation against the foothills of the Himalayas and the western TP through the low level monsoon westerlies, from April to May. The dust in the IGP region is coated with black carbon produced by local emissions and become a strong absorber of solar radiation and an efficient source of atmospheric heating [Singh *et al.*, 2004; Lau and Kim., 2006]. Both the dust and BC are forced up the Himalayan slopes by the large-scale monsoon low level flow, and by the dry pre-monsoon convection, and accumulate along the foothills of the Himalayas, with the finer particles reaching the top of the TP, and above (Lau *et al.*, 2010). The elevated dust and black carbon absorbs solar radiation and heats the atmosphere around the slopes of the TP, which further enhances the rising motion up the slopes.

The difference in temperature between 2004 and 2005 (Figure 4.(a)) shows a warming in the middle troposphere over the western TP, and a cooling near the surface of the Central Indian Plateau. This is because the Central Indian Plateau is part of a larger region that is most frequently affected by local emission and dust. The meridional wind differences (Figure 4.(a)) show the induced anomalous circulations as rising in the warming region of the southern slopes of the TP and sinking to the north in the drying region. While the difference in moisture between 2004 and 2005 (Figure 4.(b)) shows an anomalous upward transport of wet air from the lower to the upper troposphere in the western TP and Himalayas, the enhanced moisture increases convective instability, spurring deep convection over northern India. The condensation heating from deep convection amplifies the seasonal warming over the TP, resulting in a widespread upper tropospheric warming anomaly over the TP (Lau *et al.*, 2010). Overall, we find enhanced warming during the pre-monsoon season, both in the lower and middle troposphere, which is indicative of a strengthened moisture increase pattern, consistent with the EHP.

3.3 Accelerated snow melting over the TP

The enhanced warming induced by the EHP is related to accelerated snow melting over the TP and the region of most pronounced anomalous snow melt coincides with the regions of maximum surface warming. Figure 5 illustrates the difference in the snow-cover fraction (SCF) between 2004 and 2005 (2004 minus 2005) over the TP during the pre-monsoon season. The enhanced snow melting is observed at elevated altitudes over the foothills of the Himalayas and western TP during spring. The decrease in the SCF is due to both a reduction in snow cover and to the snow aging, as well as to the exposure of the underlying darker soil when the snow has melted (Lau *et al.*, 2010). Although the average elevation is higher than 4,000 m, most of the interior area of the TP has a relatively small persistence of snow cover and almost all the significant SCF negative anomaly occurs in the western TP and the Himalayas. The regions with deeper snow, (smaller areas such as the Himalayan slope), have a larger percentage reduction during March to May. The maximum reduction is approximately 50%. The relatively low effective snow cover reduction in other areas is because of the fact that a large part of the eastern TP remains snow free in June. Figure 6 shows the intra-seasonal variation of AOD, upper level temperature, snow cover, and precipitation for 27 March to 24 July. The solid lines represent the year 2004 and the dashed lines represent 2005. The time series of the high daily AOD values (yellow color) are contrasted with the variability in the snow cover fraction, which we define as “SCF averaged western TP” (Figure 6.(c)). The upper temperature level shows a greater success at capturing the variability in the snow melting time series, especially during May and July. This negative correlation is consistent with the precipitation time series in the IGP (Figure 6.(d)).

As a result, the Himalayas and western TP are characterized by accelerated snow melting in AM 2004 in comparison with AM 2005. This melting is located mainly over the Himalayas and western TP during the pre-monsoon season. When the SCF disappears earlier in the spring, the large amounts of energy that would have been directed in snow-melting, directly warm the soil. This comparison also suggests a

link between the snow cover fraction over the TP and the AOD in IGP (Figure 6.). Furthermore, aerosols modify the surface energy balance (Lee and Kim, 2011), which can also affect surface snowmelt.

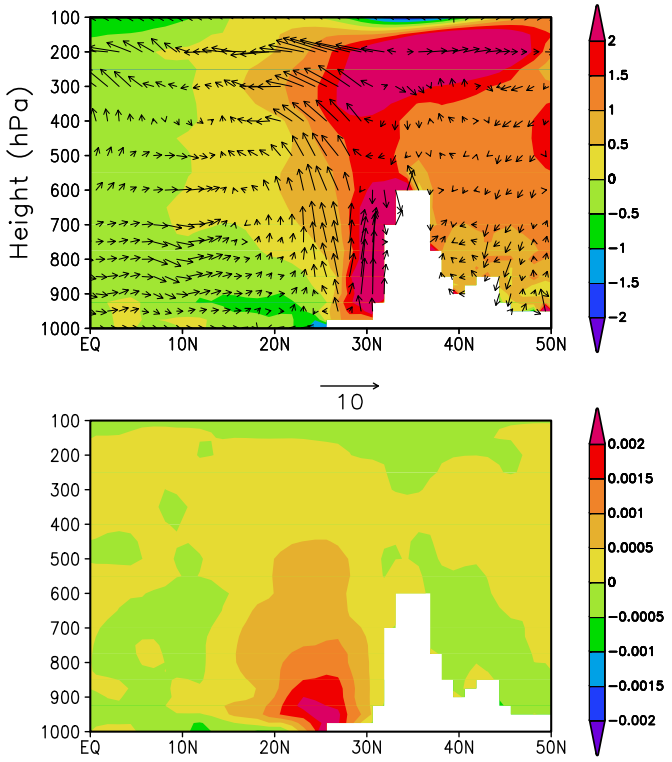

Figure 4 Latitude-height cross-section showing the difference between the years 2004 and 2005 in: a) temperature (shaded, °C) and meridional circulation(vector); and (b) specific humidity (g/kg) over IGP region (70E–100E). Units of pressure velocity and meridional wind are -10^{-4} hPa s^{-1} and ms^{-1}, respectively.

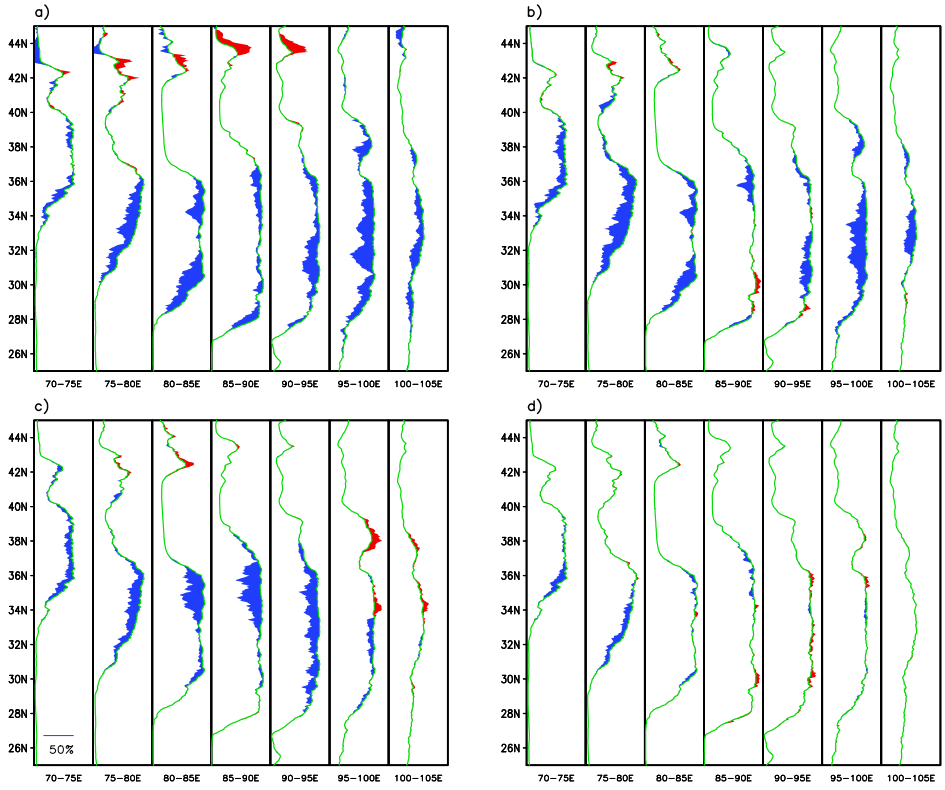

Figure 5 Map showing the difference between the years 2004 and 2005 (2004 minus 2005) snow cover (%) over the TP region for: a) March, b) April, c) May, and d) June. Blue (red) color indicates negative (positive) anomaly in 2004 relative to 2005. Green color indicates topography

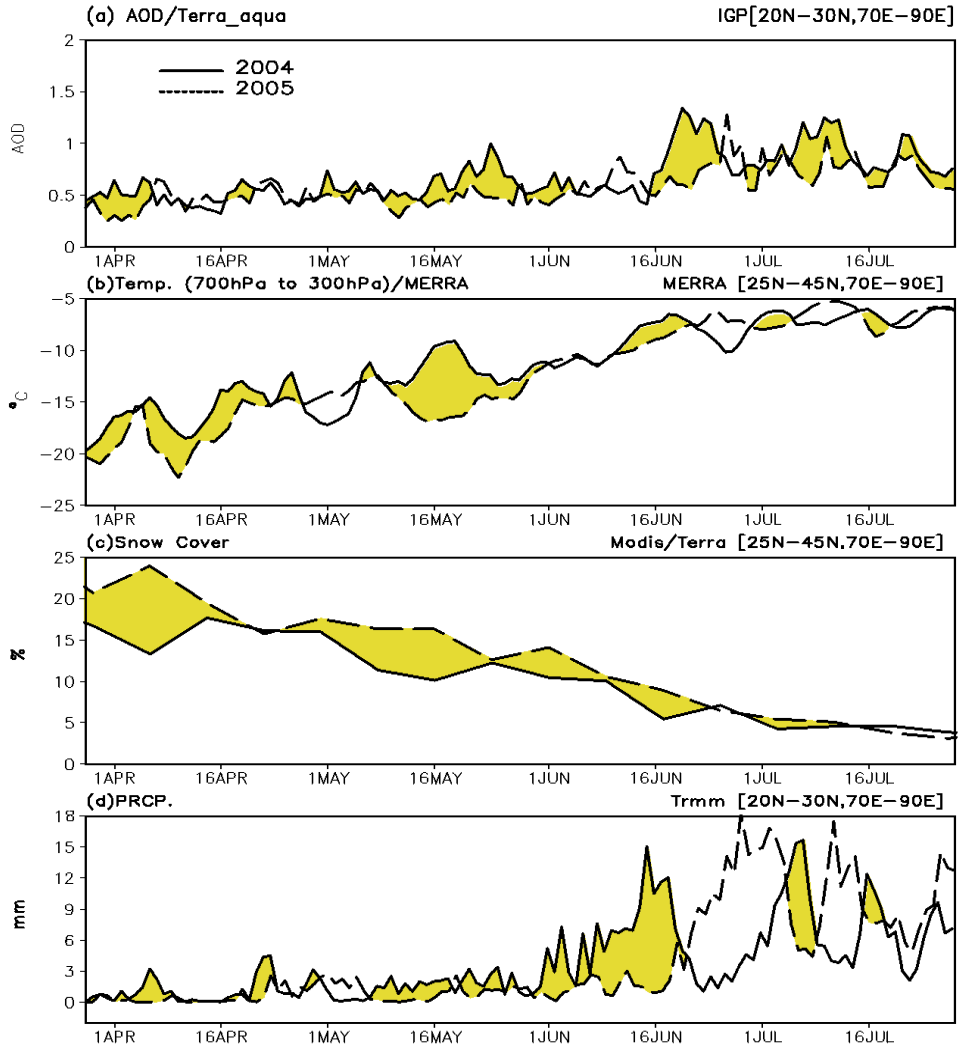

Figure 6 Time series of: a) AOD averaged over the IGP (20–30N, 70–90E), b) layer mean daily temperature (C°) between 700 and 300 hPa averaged over the western TP (25–45N, 70–90E), c) snow cover fraction (%) averaged over the Tibetan Plateau, and d) TRMM precipitation (mm day^{-1}) averaged over the IGP between 27 March–24 July. The solid lines represent the year 2004 and the dashed lines represent 2005. The yellow color denotes positive (negative) deviations from 2005 for AOD, temperature and precipitation (snow cover fraction).

4. Discussion

In an observational study, we found that the heating of the troposphere by elevated dust and black carbon aerosols in the boreal spring can lead to a widespread enhanced land-atmosphere warming, and accelerated snow melt in the Himalayas and on the Tibetan Plateau.

In 2004, the absorbing aerosol loading during the pre-monsoon season, (the most active period for dust transport and local emissions), was found to be much stronger over the IGP in comparison with 2005. The mean AOD over the IGP was 0.52 and 0.41 during the pre-monsoon periods of 2004 and 2005, respectively. Coinciding with an increase in the aerosol concentration in 2004, the difference in temperature between 2004 and 2005 indicates a warming in the middle atmosphere and on the surface over the entire TP. The vertical temperature and moisture differences between 2004 and 2005 on the southern slopes of the TP also suggest an increase in temperature (most likely related to an increase in convection). It appears, therefore, that absorbing aerosols can affect the meridional temperature gradient between the western TP and the tropical Indian Ocean.

Our results indicate that the AOD on the IGP firstly affects the Tibetan Plateau surface temperature through the EHP-related atmospheric circulation change, and then affects the snow cover fraction change. It is shown that the snow cover fraction over the TP reduces in early spring, with an increase in atmospheric heating over the Himalayas and the TP. This reduction is closely related to the significantly increased surface sensible heat flux from the atmosphere into the surface and the subsequent warming over the TP and its surrounding atmosphere, due to an increase in the preceding spring snow melting over the TP (Lau *et al.*, 2010).

Absorbing aerosol deposition over snow cover acts to reduce the snow albedo and enhances absorbed solar radiation and snow melt rates (Painter *et al.*, 2007). In addition to the enhanced tropospheric warming over the western TP and Himalayan region near the snow surface, the increasing amounts of absorbing aerosols could

enhance the effect (or work independently) in melting the Tibetan Plateau snow cover (Gautam *et al.*, 2009). Our observation results are consistent with the key features of the model results proposed by Lau *et al.*, (2010).

In summary, our results suggest that, as a response to aerosol forcing by absorbing aerosols on the Indo-Gangetic Plain, the EHP-effect may significantly accelerate snow melt during the pre-monsoon season over the TP. In addition, the absorbing aerosol anomalies may affect the Asian monsoon via the snow cover and the TP surface temperature.

PART II : Study of aerosol Effect on accelerated snow melting over the Tibetan Plateau using CMIP5 simulation data

1. Introduction

Atmospheric aerosols are of great importance to global climate because of their absorbing as well as scattering properties and in turn significantly influence the Earth's radiation budget [Ramanathan *et al.*, 2001; Haywood and Boucher, 2000; Bellouin *et al.*, 2005]. In general, aerosols could offset the greenhouse warming by directly scattering the sunlight back to space and by indirectly enhancing cloud albedo, thereby cooling the climate. Atmospheric aerosols also influence the snow cover fraction via several mechanisms.

However, absorbing aerosols heat the atmosphere because of their absorption of solar radiation, which in turn raise the greenhouse warming [Jacobson, 2001]. Therefore, absorbing aerosols such as black carbon and dust are thought to affect the hydrology and radiative forcing over Asia (Ramanathan and Carmichael, 2008; Menon *et al.*, 2002; Lau and Kim., 2007; Lee and Kim., 2010) as well as increase snow melt in snow covered regions (Jacobson, 2004; Flanner *et al.*, 2007; Koch *et al.*, 2009; Lau *et al.*, 2010; Lee and Kim., 2011).

The Tibetan Plateau (TP) is located close to regions in South and East Asia that have been and are predicted to continue to be the largest source of black soot in the world (Bond *et al.*, 2007; Ohara *et al.*, 2007). The extensive black carbon and dust aerosols could be lofted to the high TP and incorporated in snowflakes that when falling on the glaciers darken their surface, which has led to initial studies of the amount BC in the snow and ice of Himalayan glaciers (Flanner *et al.*, 2007). Etienne et al (2007) showed that 915km^2 of Himalayan glaciers thinned by an annual average of 0.85cm between from 1994 and 2004.

Recently, a model study by Lau et al (2010) showed that the heating of the

troposphere by elevated dust and black carbon aerosols in the boreal spring can lead to widespread enhanced warming of the land-atmosphere, and accelerated snow melt in the Himalayas and western TP region. The snow cover of the Tibetan Plateau and Himalayas is very important for the regional climatic change and hydrological cycle. In recent years, there have been growing evidences of increased warming, accompanied by early snow melt, and retreat of high mountain glacier in the Himalayas and the TP regions (IPCC, 2007; He *et al.*, 2003; Jain, 2008; Ren *et al.*, 2006; Kulkarni et al 2007).

Up to now, most studies about snow melt in the Himalayas and TP are focused on greenhouse warming (Duan et *al* 2006, Oerlemans 2005, Kulkarni *et al* 2002, Jiawen 2006). Yet, the greenhouse warming rate is of the order of 0.1-0.15K/decade, While the warming of the TP has been estimated to be much faster, at 0.32K/decade(Liu and Chen, 2000). Over Himalaya foothill regions and Middle Mountain regions in Nepal, the warming rate is even faster, estimated at 0.7-1.2C per decade since 1977-94 (Shresth at el., 1999). Based on these differences in warming rates, it is not difficult to surmise that global warming is not the sole agent of change in these regions, and that local forcing and feedback processes are likely to play an important role in causing the faster warming rate, and accelerated retreat of the mountain glaciers.

Many factors besides greenhouse warming could have led to accelerated warming over the Himalayas and TP. These include increased land-use and land change, increased sunlight duration from reduction in cloudiness, increased water vapor feedback, and reduction of snow albedo by deposition of soot and dust on snow surface (Kang *et al* 2000, Prasad and Singh 2007, Flanner *et al* 2007, 2009, Yasunari *et al* 2009). Recently Ramanathan *et al* (2007) estimated that atmospheric heating by Asian Brown Clouds (ABC) doubles the greenhouse warming over South Asia, and may contribute substantially to the loss of glacier mass in the Himalayas. Also, absorbing aerosol induced reduction of snow cover/albedo and its contribution to snow/ice retreat have only begun to receive attention, so there is a need for more extensive coupled modeling data, such as CMIP5 simulations.

In this article, we investigate the impact of atmospheric heating by aerosol in boreal spring in possibly leading to enhanced pre-monsoon surface warming and early snow melt in the Himalayas and TP region using CMIP5 model simulation. Our analysis focuses on the change of spring time snowpack over the TP and their subsequent impacts on surface radiative flux change.

2. Data and Methodology

2.1 observation data

For model evaluations, Moderate Resolution Imaging Spectroradiometer (MODIS) is a 36-channel visible-to-thermal-infrared sensor that was launched as part of the EOS Terra payload on December 18, 1999. Various snow and ice products are produced with MODIS imagery and the data are available at a variety of spatial and temporal resolution (Hall *et al.*, 2001). The quality of MODIS snow data has been evaluated (e.g., Pu *et al.*, 2007) and results indicate that the overall accuracy is about 90% over the the TP region. In this study, a preliminary version of the gridded global monthly snow cover product MOD10CM is used, ata 0.05° resolution covering March 2000 to 2011. The most challenging task in the compiling of monthly files was the correct handling of missing values in the daily product, MOD10 Level 2 from which the monthly values are derived. Theerosol optical depth has been obtained using Level-3 MODIS gridded atmosphere monthly global product 'MOD08_M3'(ESDT Long Name: MODIS/Terra Aerosol Cloud Water Vapor Ozone Monthly L3 Global 1Deg CMG). The monthly average MOD08_M3 product files are produced at a spatial resolution of 1 degree by 1 degree. The Atmospheric Infrared Sounder (AIRS) is on board NASA's Earth observing system satellite Aqua (EOS-Aqua). The geophysical parameters have been averaged and binned into 1°x1° grid cells, from -180.0° to +180.0° longitude and from -90.0° to +90.0° latitude. AIRS provides several atmospheric parameters, including vertical profiles of atmospheric temperature. The accuracy of temperature

and water vapor profiles is expected to be 1 K for 1 km levels and 15% for 2 km layers in the troposphere, respectively (Tobin *et al.*, 2006). In this study we use the AIRS Level 3 Monthly Gridded Retrieval Product.

For wind, we use the reanalysis data from Modern Era Retrospective-analysis for Research and Applications (MERRA) (Kim *et al.*, 2006). This study uses a standard monthly mean output that is provided on 42 pressure levels at a horizontal resolution of 1.25° latitude × 1.25° longitude for the period 2000-2011.

2.2 Model description

The results of this paper are based on coupled atmosphere-ocean global climate model (CSIRO-Mk3.6) with dynamical sea ice and soil canopy scheme with prescribed vegetation properties (Gordon *et al.* 2002, 2010). The CSIRO-Mk3.6 has an approximately 1.875°x1.875° horizontal resolution, 18 vertical levels, and is coupled on version 2.2 of the Modular Ocean Model (Gordon *et al.*, 2010).

This model is the inclusion of an interactive aerosol scheme, which treats sulfate, dust, carbonaceous aerosol, and sea salt. The radiation scheme treats the direct effects of all these aerosol species on shortwave radiation and the effects of dust on longwave radiation. The indirect effects of sulfate, carbonaceous aerosol and sea salt on liquid-water clouds are also included, via an empirical parameterization of cloud droplet concentration as a function of aerosol number concentration (Rotstayn *et al.*, 2012). The model simulations are based on the CMIP5 experimental design (Taylor *et al.*, 2009, 2012); (see http://cmip-pcmdi.llnl.gov/cmip5/ for further information about CMIP5 forcing data). Anthropogenic forcing agents in these model runs are long-lived GHGs, ozone and aerosols (changes in land use are not included).

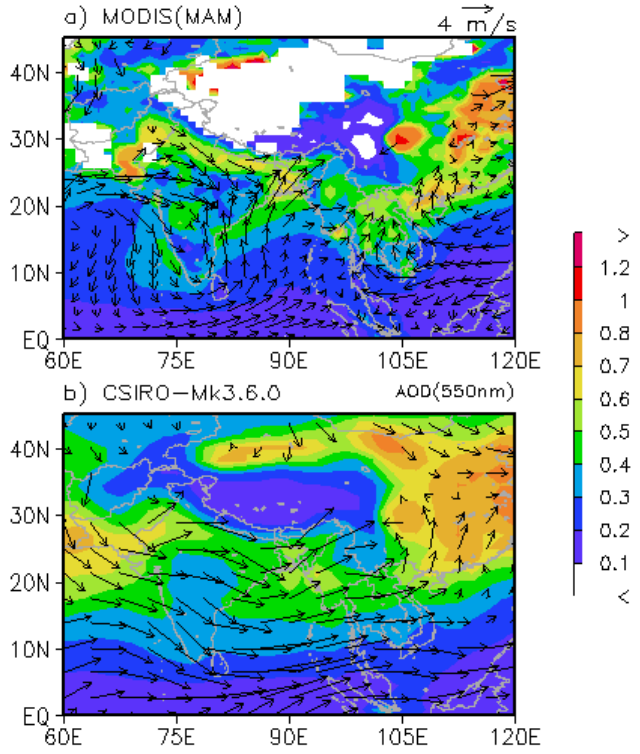

Figure 7 Aerosol optical depth(shading) and 850 hPa wind(vector) averaged for March-April-May(MAM) over the Tibetan Plateau, (top) MODIS and (bottom) Model.

The CSIRO-Mk3.6 prescribed by CMIP5-recommended, annual-mean concentrations of long-lived GHGs (carbon dioxide, methane, nitrous oxide and chlorofluorocarbons), and monthly mean, spatially varying ozone concentrations. Emissions of anthropogenic aerosols and aerosol precursors also followed CMIP5 recommendations (Lamarque *et al.*, 2010). In addition to the direct effects and indirect aerosol effects on liquid-water clouds, the model also includes a simple treatment of the effect of black carbon on snow albedo (Hansen and Nazarenko, 2004). The anthropogenic-forcing data sets are prescribed for both the historical period and the four Representative Concentration Pathways (RCPs); see Moss *et al.* (2010) for an overview of the RCPs. The model includes the historical time series of annual-mean total solar irradiance recommended

for CMIP5; this includes estimates of both the 11-yr solar cycle and changes in background irradiance (Lean, 2000; Wang *et al.*, 2005). CMIP5 does not specifically include a prescribed data set for volcanic forcing. Therefore, zonally averaged distributions of stratospheric sulfate are prescribed based on Sato *et al.* (1993). Stratospheric sulfate is distinct from the (time-invariant) source of sulfur from continuously erupting volcanoes in the model's tropospheric sulfur cycle.

To identify the mechanism of forcing agents, three sets of five-member ensemble experiments are used, first with all forcing (HIST), second without aerosol forcing (NoAA), and third with only long-lived greenhouse gases (GHGs), for 55 years from 1951 to 2005. Rostayn *et al.* 2012 suggested that aerosols act against a background of GHG-induced warming, it is believed that an approach using HIST minus NoAA could provide a more reliable simulation. Therefore, we use the difference between HIST and NoAA (AERO) to investigate the aerosol-induced snow cover fraction. A Student's t-test has been used to assess the statistical significance of all trends.

3. Results

3.1. Model evaluation

To evaluate the impacts of aerosol-induced snow cover change, it is important to assess the climatological features of simulated climatic variables; particularly the snow cover fraction (SCF), surface air temperature and aerosol optical thickness. During the pre-monsoon season, in March-April and-May, aerosols from local sources, biomass and biofuel burning, and dust transport rapidly build up on the Indo-Gangetic Plane(IGP : 70-90°E, 25-32°N). Dust aerosols are transported from deserts (Pakistan/Afghanistan, Middle East, Sahara, and Taklamakan) adjacent to the Asian monsoon region accumulate to high elevation against the foothills of the Himalayas and western TP through low level monsoon westerly (Figure 7), during MAM. The

dusts in IGP region are coated with black carbon produced from local emissions and become a strong absorber of solar radiation and efficient source of atmospheric heating [Singh *et al.*, 2004; Lau and Kim., 2006].

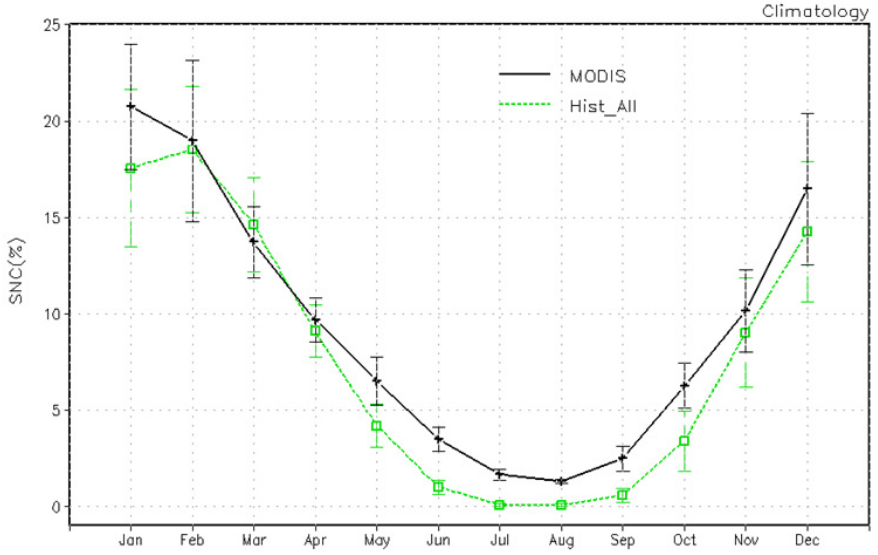

Figure 8 Monthly snow cover fraction(%) from MODIS and model(green line).

The highest measurement of AOD(>0.7) from CSIRO-Mk3.6, is over northeastern China. In comparison with the observed AOD from the moderate resolution imaging spectro-radiameter(MODIS), the AOD of the model has a resonable spatial distribution over India, and around the slopes of the TP. However, the model, appears to have underestimated the AOD over the IGP(Figure 7). The interior of the TP has a bright surface and the readings of AOD form MODIS are not included due to their high uncertainty. Figure 8 shows the monthly mean SCF from both the model and MODIS. The observation shows approximately 25% of annual variation are covered by snow during winter and spring over the TP. Remarkable changes in the SCF occur between February and June, but the changes are slight between July and October. The model underpredicts SCF by 3% in the warm season probably due to its coarse horizontal

resolution and smooth terrain, and it therefore fails to capture the lasting snowpack at a high elevation(>4000m) during the summer (Qian *et al.*, 2011).

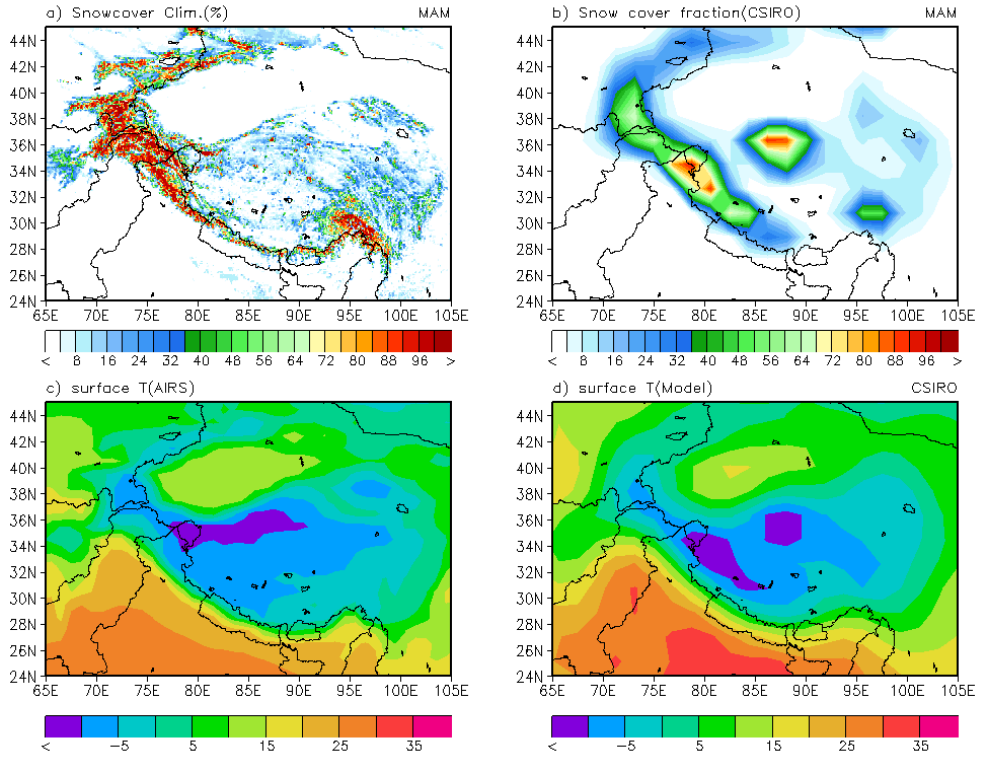

Figure 9 Spatial distribution of March-April-May(MAM) mean observed climatology of: (a) MODIS snow cover fraction (from2000 to 2011) and (c) air temperature(°C) from AIRS, compared with the corresponding climatology of the model of (b) snow cover fraction(%) and (d) surface air temperature from the historical run over the Tibetan Plateau.

The areas of most persistent snow cover (i.e. SCF >70%) are located in the Himalayas, and the western part of the TP, but there is less SCF over the interior area of the TP, even though the average elevation is above 4500m (Figure 9a). The CSIRO-Mk3.6 remakably underestimates the SCF, especially over the eastern part of the TP. The model fails to capture the complex domain that generates the observed spatial pattern due to its coarse spatial resolution. However, the model simulates

a reasonable seasonal variation of the SCF in the TP, but under-estimates the SCF by about 3% (Figure 7).

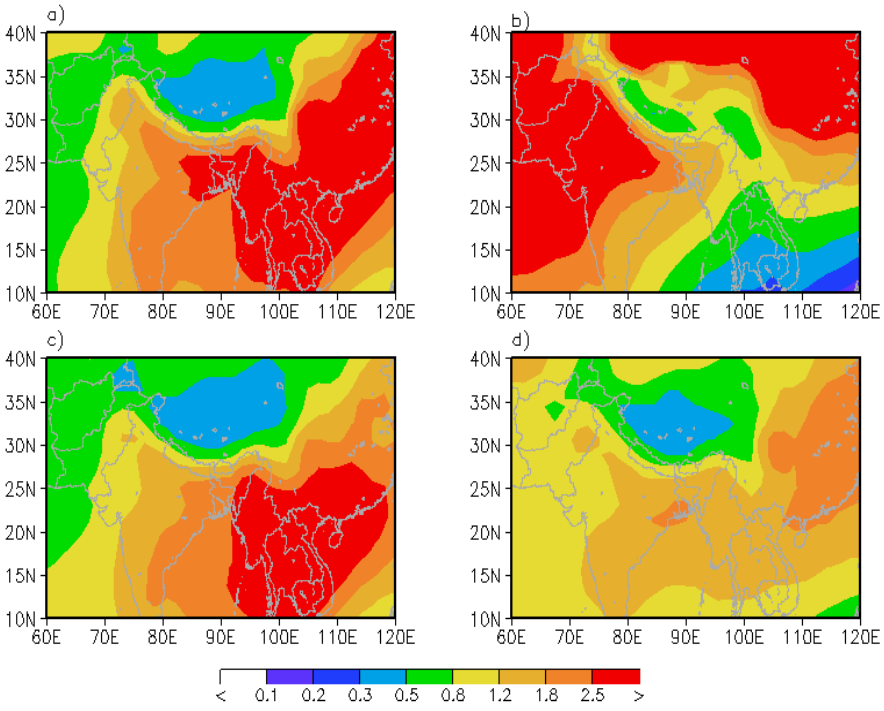

Figure 10 MAM mean atmosphere mass content of a) black carbon (10^{-6} kg m^{-2}), b) dust(10^{-4} kg m^{-2}), c) OM(10^{-5} kg m^{-2}), and SO_4(10^{-5} kg m^{-2})

The surface air temperature climatology simulated by the model (HIST) shows a temperature difference of over 40°C between the interior TP and the IGP, with a large gradient along with slope of the TP. The model's distribution of surface air temperature is similar to the surface air temperature from the atmospheric infra-red sounder (AIRS), except for the area at the top of the TP. The broad similarity between the model's SCF, AOD, and surface air temperature with those of observations, provide assurance of the realism of the model's simulations.

3.2. Aerosols effects on snow melt

In this section we compare the results of the CSIRO-Mk 3.6 global climate simulations with the set of 5-member individual-forcing historical ensembles; all forcong (HIST), aerosol forcing (AERO), without aerosol forcing (NoAA), and green house gase forcing (GHG), to investigate the relative importance of the relevant agents on the surface energy and water budgets over TP. The following analyses focus on aerosol radiative forcing and temperature, snow cover fraction, and rainfall changes induced by the forcing from each ensemble. These variables are the most relevant to the hydrological cycle.

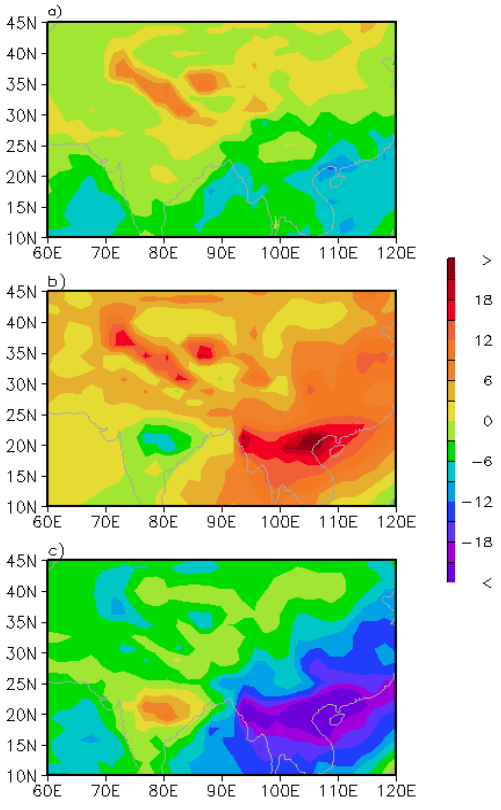

Figure 11 Anthropogenic aerosol forcing(the difference between 2000 and 1850) in W m^{-2} during MAM, calculated as the total aerosol radiative flux perturbation a) at top of atmosphere(TOA), b) in the atmosphere, and c) at the surface.

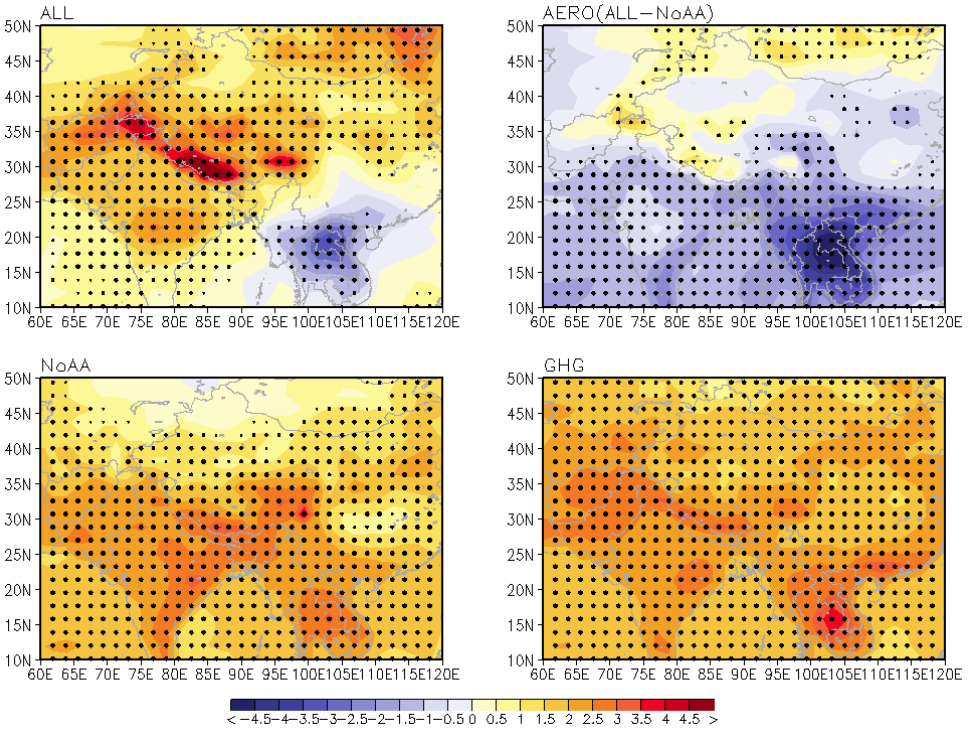

Figure 12 Spatial distribution of surface air temperature (K century^{-1}) for the years 1951-2010, during MAM, from: a) All forcing, (b) All minus NoAA (aerosol forcing), (c) without aerosol, and (d) GHG. Regions passing the 90% significance level are high-lighted by stipple. Significance is assessed through the t-value of ensemble trend.

Figure 10 shows the spatial distribution of the mass atmospheric content of black carbon, dust, organic matter and SO_4 by the mode, respectively. The spatial distribution of black carbon (BC) and organic mater (OM) resemble each other very closely, and follow the proportion of BC and OM in emissions from fossil fuel and biomass burning. Dust particles from the Thar desert are transported over the IGP and the western India(Liu *et al.*, 2005). These are strongly transported vertically and dust particles emitted from Asian sources are lifted efficiently to 8 km [e.g., Merrill *et al.*, 1989; Ginoux *et al.*, 2001].

To further investigate the effects induced by aerosols, Figure 11 shows the spatial

distribution of aerosol radiative forcing (ARF) at the top of the atmosphere (TOA), within the atmosphere (top minus surface), and at the surface during MAM, respectively. The CMIP5 experimental design (Taylor *et al.*, 2009) includes simulations designed to calculate an estimate of the radiative forcing due to anthropogenic aerosols. The method is based on two 30-yr atmospheric runs with prescribed SSTs and sea-ice taken as climatology from the pre-industrial control run. One run uses 1850 aerosol emission data and the other uses emissions for the year 2000. The difference in the amount of radiation between the two runs gives an estimate of anthropogenic aerosol forcing (Rotstayn *et al.* 2012).

The magnitude of ARF at the TOA is much smaller than that in atmosphere, except for TP region. This is because the negative forcing (cooling) due to aerosol scattering is adjusted by aerosol absorption (warming). As a result, the spatial pattern of ARF is similar to that at the surface but with opposite sign, implying that the net effect of regional aerosols is to redistribute heat between the surface and the atmosphere. The spatial distribution of ARF shows that the distribution of radiative flux anomalies is similar to the atmosphere mass content of aerosols, except for over the TP, where aerosols are not abundant. The atmospheric heating is mainly due to the contribution of black carbon and organic matter over South Asia and the IGP, where the ARF in the atmosphere is around 15-18W/m^2. Even though the atmospheric mass content of black carbon is almost 10 times smaller than dust, the former plays a very important role in absorbing solar radiation in the atmosphere, especially over Tibetan Plateau (Kim *et al.*, 2006). This indicates the sum of direct and indirect (first and second) effect, plus the effect of snow darkening. The ARF pattern is more consistent with the trends of SCF indicating a stronger atmospheric heating influence from aerosols, especially BC and dust.

Figure 12 shows the ensemble-mean surface air temperature for the four cases of HIST, aerosol-induced effect (AERO), NoAA, and GHG for MAM, respectively. The distribution of surface air temperature by HIST (Fig. 6a) shows evidence of an increasing surface air temperature over parts of the TP and India region. The surface air temperature increases significantly at a level of 90% over most of Asia and the

entire TP , and the warming trend is at a rate of more than 3°C/100yr over the western TP. However, HIST shows a decreasing surface air temperature over Southeast Asia caused by anthropogenic aerosol forcing (Fig. 6b). The aerosol-induced effect in MAM also shows a tendency for increasing surface air temperatures over the TP. This warming trend appears to be consistent with observation results in response to regional forcing from IGP aerosols (Lee *et al.*, 2010), as atmospheric aerosols have more complicated effects on surface air temperature change. Aerosols scatter and absorb solar radiation, thereby reducing the amout of radiation reaching the surface and causing cooling. Thus, the remarkable cooling trend over South Asia and India is associated with BC, OM and dust aerosols (Figure 10). However absorbing aerosols, especially carbonaceous aerosols and dust aerosols absorb solar radiation and heat the atmosphere. Thus we can see that the surface air temperature trend increases (significant at 90% confidence level) by more than 1°C/100yr over the TP and the northern part of the region. As the regions of warming are not near the centers of high AOD, the warming trend cannot, however, be attributed to direct aerosol radiative forcing alone, but rather arises from an atmospheric feedback process and snow darkening effect. During the pre-monsoon season, dust is transported from the deserts west of the Indian subcontinent, where it accumulates over the IGP against the foothills of the Himalayas (Lau and Kim., 2006). As dust storms pass through the IGP, the dust aerosols sweep up BC from local emissions in the IGP, creating highly-absorbing dust particles (Eck *et al* 2005). Both the dust and BC are piled up on the Himalayas slopes via emissions from India, and accumulate along the foothills of the Himalayas, with the finer particles reaching the top of the TP, and above. As suggested by Lau *et al.*(2010), the elevated dust and black carbon absorbs solar radiation and heats the atmosphere over the TP; decreasing the snow albedo around the slopes of the TP.

The surface air temperature increases significantly by 90% over all regions. In relation to “GHG”. This warming trend translates to more than 2°C/100yr over areas of South Asia and the TP. It should be noted that the temperature change induced by “GHG” and aerosols (“HIST minus NoAA”) is not a linear combination of the effects

induced by each forcing mechanism (as shown in Figure 12b-d). The warming trend over the TP in Figure 6a is larger than the warming induced by "without aerosols (NoAA) " (Figure 12c), and by "GHG" (Figure 12d). Although the temperature rise related aerosols (HIST minus NoAA) is minimal over the TP, for an explanation of the faster warming of the TP, aerosols need to be considered.

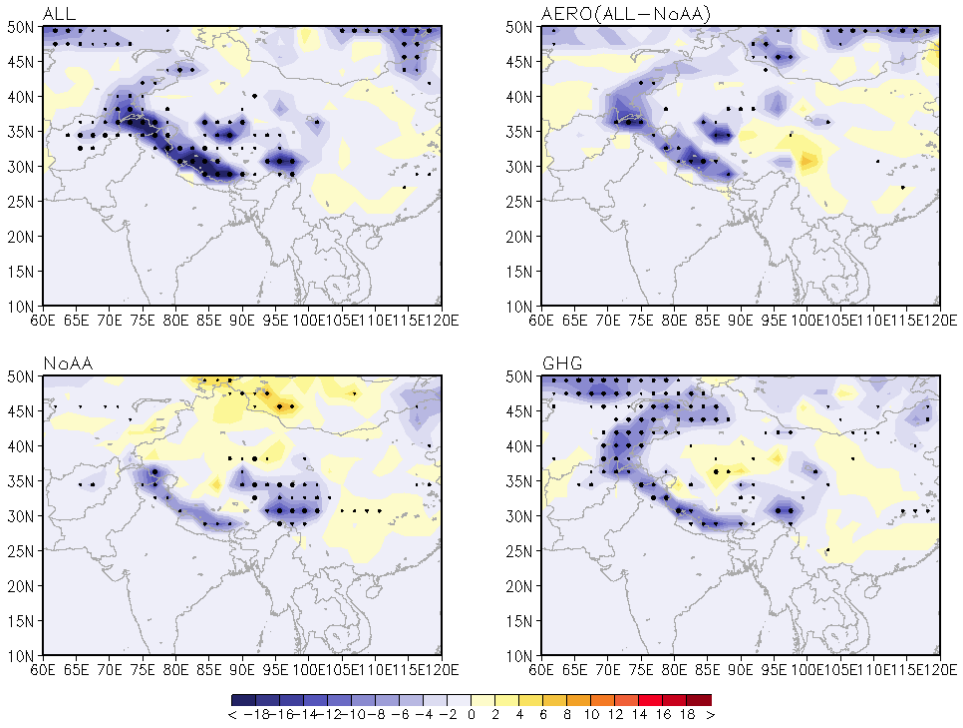

Figure 13 Spatial distribution of snow cover trends(% century^{-1}) for the years 1951-2010, during MAM from a) All forcing, (b) All minus NoAA (aerosol forcing), (c) without aerosol, and (d) GHG. Regions passing the 90% significance level are high-lighted by stipple. Significance is assessed through the t-value of ensemble trend.

Figure 13 shows the spatial distribution of the MAM SCF change usinf the different sensitivity experiments (HIST, AERO, NoAA, and GHG as discussed). With all forcing (HIST), the SCF decreases significantly by 14-18% over the western TP. In case of without aerosol forcing (NoAA), the SCF changes are very small over the western

TP (about 6%). In the case of GHG, the pattern of the SCF trend is similar to that of HIST, except for in the northern part of the interior TP, but with a smaller magnitude and with the maximum reduction of SCF around at 8-10% over the Himalayas. With HIST minus NoAA (Figure 13b), a more significant reduction of SCF can be found over the western TP and the Himalayas. There is a larger decrease trend in SCF over the TP, with a maximum reduction of SCF of around 12-15% over the western TP and the Himalayan slope. The decreased snow albedo, due to BC/dust deposition, further accelerates snow melt. As the SCF did not alter radically during "NoAA" simulation, this can be attributed to the effect of aerosol on the albedo.

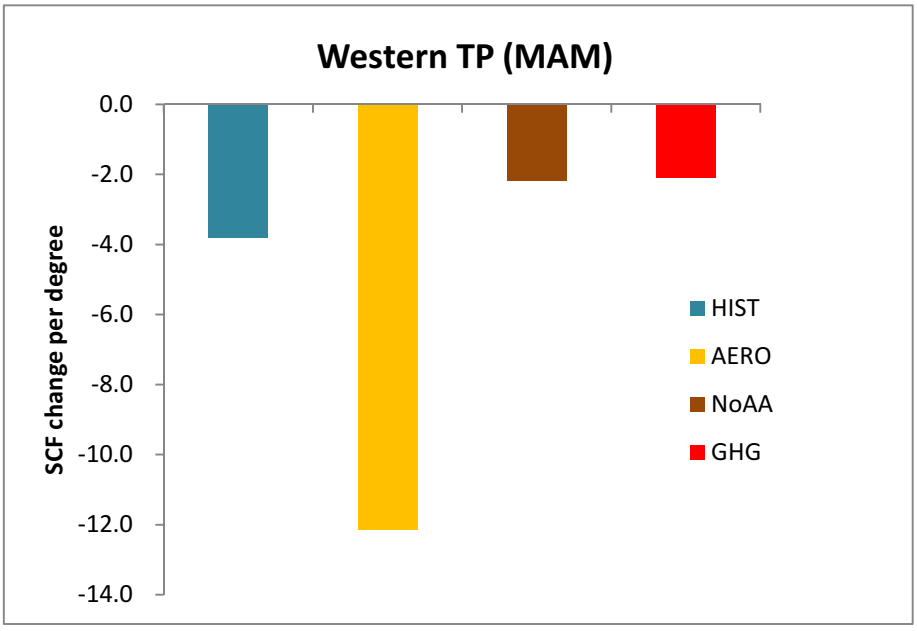

Figure 14 Rations of SCF trend against per unit degree of warming trend, during MAM, induced by HIST, AERO, NoAA, and GHG over the western Tibetan Plateau. The unit is in %/°C 100yr.

It is interesting to note that the SCF reduction induced by aerosol is more significant than that induced by GHG over the western TP. This decreased SCF trend is mainly located over the Himalayas and the western TP during the pre-monsoon season, although the trend of an increase in the surface air temperature induced

by an increase in CO_2 is larger than that induced by aerosols during MAM.

Here we calculated "the efficacy of snowmelt" as the snow cover reduction trend per unit degree of warming trend induced by HIST, AERO, NoAA, and GHG forcing. Figure 14 shows the SCF trend for unit degree of surface air temperature trend induced by HIST, AERO, NoAA, and GHG over the western TP [20-40°N, 70-90°E], respectively. The efficacy of snowmelt induced by HIST minus NoAA is about three times larger than that of HIST and five to six times larger than the increase in CO_2 during MAM. This is because a darker snow surface related directly to aerosol deposition absorbs additional shortwave radiation, and the SCF by aerosols melts faster than that by GHG (Figure 15). Therefore the increased solar radiation at the surface due to aerosol forcing melts the snow more efficiently than snow melt due to warming in the atmosphere.

In relation to the subject of snow cover reduction induced by aerosol forcing, we calculated the total cloud amount (CLD), sensible heat (SH) flux, latent-heat (LH) flux, net short-wave (SW) flux, and net longwave (LW) flux (Figure 15). The anomalous net shortwave and net long-wave fluxes at the surface are closely linked to the variation in the amount of total cloud. In March, cloud cover is reduced by the semi-direct effects of aerosol, and surface warming by downward short-wave radiation is enhanced with a simultaneous increased cooling by long wave radiation is transferred indirectly to the snow (Qian *et al.*, 2011). In addition, aerosol deposited on snow reduces surface albedo and the surface incident shortwave radiation is then also increased.

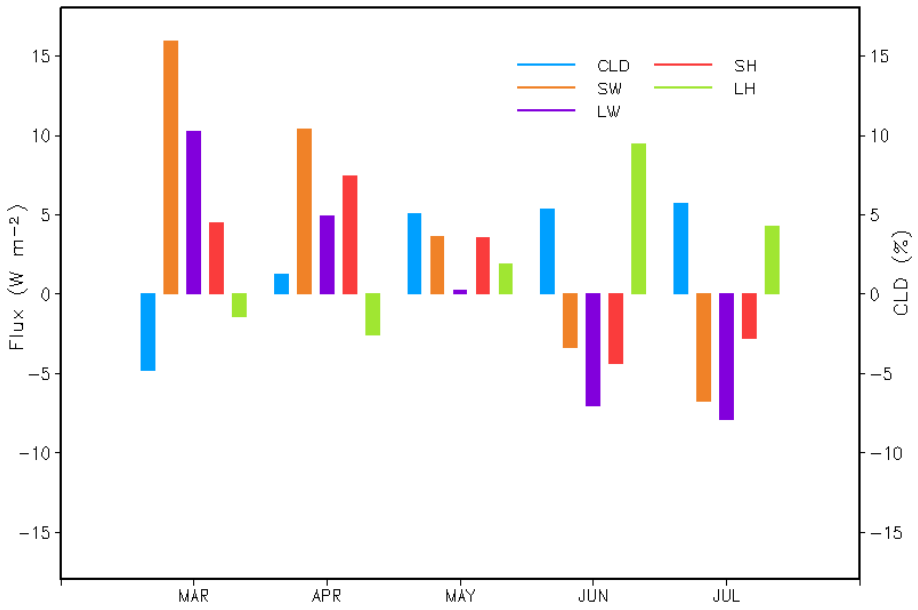

Figure 15 Monthly total cloud amount (blue line), net short-wave flux (orange), net long-wave flux(purple), sensible heat flux (red), and latent heat flux(green) differences between HIST and NoAA over the Tibetan Plateau.

We can see a remarkable increase in SH during March-April and -May due to surface warming induced by aerosol forcing, with maximum increase in SH of 7 W m^{-2} in April. During May-June and-July, the increased LH due to wetter soil induced by accelerated snowmelt warms the air and enhances the deep convection over the TP, resulting in more CLD over the TP, which then further invreases the LH. This is a time-lagged and positive feedback process.

In summary, the aerosol induced decrease in the SCF causes the land surface to absorb more solar radiation, thereby increasing the surface air temperature. As a result of the ARF in the atmosphere and the subsequent warming, the reduction in the SCF from semi –and -direct effects further decreases the surface albedo over the entire TP. The decrease in surface albedo is due to both a reduction in SCF and to snow aging, as well as to the exposure of the underlying darker soil when

the snow becomes melt(Lau *et al.*, 2010). The increased LH, due to the accelerated snowmelt, warms the air and enhances deep convection over the TP, resulting in greate CLD over the TP, which then results in a greater increase of the LH.

4. Summary and discussion

The spring snow melts from the Tibetan Plateau and Himalayan is necessary to the livelihood of the downstream populated IGP. In addition to the large pollution comprising of soot, sulfate and organic matter, the IGP has long been recognized to be strongly affected by dust transport from deserts (Pakistan/Afghanistan, Middle East, Sahara, and Taklamakan).

In this study, the CSIRO-Mk3.6 coupled climate model was used to evaluate the relative impacts of various radiativeforcings on SCF from 1951 to 2005. Anthropogenic aerosols typically follow the time series of the prescribed CMIP5 emissions, increasing rapidly from 1950, peaking in the period 1980–2005. The SCF and surface air temperature are well reproduced by CSIRO-Mk3.6 models for the historical, and in particular the annual cycle of SCF in TP seems to be well reproduced. Trend analysis of different forcing agents showed that MAM SCF has undergone significant reduction over TP. Also, we found that the heating of the troposphere by aerosols in MAM can lead to accelerated snow melt in the Himalayas and western TP. The warming and snow melt induced by aerosol are most pronounced in the western TP, where the climatological snow cover fraction is deeper (over 70%). Our estimate aerosol effect on snow melting is high, or comparable to the effect of GHG on snow, due to the decreased snow albedo induced by BC/dust deposition which can further accelerate snow melt over the TP.

The efficiency of snowmelt, defined as the snow reduction trend per unit degree of warming trend by the each forcing agent, is about 3 times larger for AERO than HIST and 5-6 times larger for AERO than CO_2 increase case during MAM, indicating

that aerosol more efficiently accelerates snowmelt because the increased solar radiation radiation induced by reduced albedo melts the snow more efficiently than snow melt due to warming in the air. A surface energy balance analysis shows that surface warming due to absorbing aerosol causes early snow melting and further increases surface-atmosphere warming through snow/ice albedo feedback.

In summary, our results suggest that, as a response to aerosol forcing by absorbing aerosol in the Indo-Gangetic Plain, the snow albedo effect may significantly accelated snow melt during pre-monsoon season over the TP. In addition to, aerosols may affect the Asian monsoon via the snow cover and the TP surface temperature. In other words, both atmospheric heating and snow darkening effect may accentuate greenhouse warming, leading to accelerated snow melting. For furure work, the aerosol effects on snow melting need to included in a high-resolution climate model such as Coordinated Regional Climate Downscaling Experiment (CORDEX) capable of resolving the complex terrains over TP regions.

REFERENCES

Bellouin, N., O. Boucher, J. Haywood, and M. S. Reddy (2005), Global estimate of aerosol direct radiative forcing from satellite measurements, Nature, 438, 1138–1141.

Bond, T. C., E. Bhardwaj, R. Dong, R. Jogani, S. Jung, C. Roden, D. G. Streets, and N. M. Trautmann (2007), Historical emissions of black and organic carbon aerosol from energy-related combustion, 1850–2000, *Global Biogeochem. Cycles*, 21, GB2018, doi:10.1029/2006GB002840.

Dey, S., S. N. Tripathi, R. P. Singh, and B. N. Holben (2004), Influence of dust storms on the aerosol optical properties over the Indo-Gangetic basin, *J. Geophys. Res.*, 109, D20211, doi:10.1029/2004JD004924.

Flanner, M. G., C. S. Zender,, P. G. Hess, N. M. Mahowald, T. H. Painter, V. Ramanathan, and P. J. Rasch: Springtime warming and reduced snow cover from carbonaceous particles, Atmos. Chem. Phys., 9, 2481-2497, 2009.

Ginoux, P., Chin, M., Tegen, I., Prospero, J. M., Holben, B., Dubovik, O., and Lin, S.-J.: Sources and distributions of dust aerosols simulated with the GOCART model, J. Geophys. Res., 106, 20255–20274, 2001.

Gordon, H. B., Rotstayn, L. D.,McGregor, J. L., Dix, M. R., Kowalczyk, E. A., O'Farrell, S. P., Waterman, L. J., Hirst, A. C., Wilson, S. G., Collier, M. A., Watterson, I. G., and Elliott, T. I.: The CSIRO Mk3 Climate System Model, Technical Paper No. 60, CSIRO Atmospheric Research, Aspendale, Vic., Australia, 134 pp., available online at: http://www.cmar.csiro.au/e-print/open/gordon 2002a.pdf, 2002.

Gordon, H. B., O'Farrell, S. P., Collier, M. A., Dix, M. R., Rotstayn, L. D., Kowalczyk, E. A., Hirst, A. C., and Watterson, I. G.: The CSIRO Mk3.5 Climate Model, Technical Report No. 21, The Centre for Australian Weather and Climate Research, Aspendale, Vic., Australia, 62 pp., available online at: http://www.cawcr.gov.au/publications/technicalreports.php, 2010.

Hansen, J., and L. Nazarenko, 2004: Soot climate forcing via snow and ice albedos. Proc. Natl. Acad. Sci., 101, 423-428, doi:10.1073/pnas.2237157100

Haywood, J., and O. Boucher (2000), Estimates of the direct and indirect radiative forcing due to tropospheric aerosols: A review, Rev. Geophys.,38, 513–543.

He Y, Z. Zhang, W. H. Theakstone, T. Chen, T. Yao, and H. Pang (2003) Changing features of the climate and glaciers in China's monsoonal temperate glacier region *J. Geophys. Res.* 108(D17) 4530, doi:10.1029/2002JD003365

IPCC, 2007 Climate Change 2007: The Physical Science Basis. Contribution of Working Group I to the Fourth Assessment Report of the Intergovernmental Panel on Climate Change [Solomon, S., D. Qin, M. Manning, Z. Chen, M. Marquis, K.B. Averyt, M.Tignor and H.L. Miller (eds.)]. Cambridge University Press, Cambridge, United Kingdom and New York, NY, USA.

Jacobson M.Z. (2004). Climate response of fossil fuel and biofuel soot, accounting for soot's feedback to snow and sea ice albedo and emissivity. *J. Geophysica Research* 109: doi:10.1029/2004JD004945

Jain S. K. (2008) Impact of retreat of Gangotri glacier on the flow of Ganga River *Current Science* 95(8) 1012-1014

Kim, G.-K., I. Stajner, and J. Chen, 2006: NASA's Modern Era Retrospective-analysis for Research and Applications. U.S. CLIVAR Variations, 4 (2), 5-8.

Kim, M.-K., W. K. M. Lau, M. Chin, K.-M. Kim, Y. C. Sud, and G. K. Walker (2006), Atmospheric teleconnection over Eurasia induced by aerosol radiative forcing during boreal spring, J. Clim., 19, 4700–4718, doi:10.1175/JCLI3871.1.

Koch, J., B. Menounos, and J. J. Clague. Glacier change in Garibaldi Provincial Park, southern Coast Mountains, British Columbia, since the Little Ice Age. Global and Planetary Change, 66: 161-178, 2009.

Kulkarni, A. V., I. M. Bahuguna, B. P Rathore, S. K. Singh, S.S. Randhawa, R. K. Sood and S. Dhar (2007) Glacial retreat in Himalaya using Indian remote sensing satellite data *Curr. Sci.*92(1) 69-74

Lau, K.-M. and K.-M. Kim. (2006) Observational relationships between aerosol and Asian monsoon rainfall, and circulation *Geophys. Res. Lett.* 33 L21810, doi:10.1029/2006GL027546

Lau, K.-M, M.-K. Kim, K.-M. Kim and W-S. Lee. (2010): Enhanced surface warming and accelerated snow melt in the Himalayas and Tibetan Plateau induced by absorbing aerosols. Environmental Research Letter 5, 025204.

Lee, W. S., and M. K. Kim. (2010) Effects of radiative forcing by black carbon aerosol on spring rainfall decrease over Southern Asia. Atmos. Environ., 44, 3739-3744

Liu, X., J. E. Penner, and M. Herzog. (2005). Global modeling of aerosol dynamics: Model description, evaluation, and interactions between sulfate and nonsulfate aerosols, J. Geophys. Res., 110, D18206, doi:10.1029/2004JD005674.

MODIS (2004). http://daac.gsfc.nasa.gov/MODIS/Terra/atmosphere/MOD08_M3.shtml

Merrill, J.T., Uematsu, M., Bleck, R., 1989. Meteorological analysis of long-range transport of mineral aerosol over the North Pacific. J. Geophys. Res. 94, 8584–8598.

Ming, J., H. Cachier, C, Xiao, D. Qin, S. Kang, S. Hou, and J. Xu: Black carbon record based on a shallow Himalayan ice core and its climatic implications, Atmos. Chem. Phys., 8, 1343-1352, 2008.

Ohara, T., H. Akimoto, J. Kurokawa, N. Horii, K. Yamaji, X. Yan, and T. Hayasaka. An Asian emission inventory of anthropogenic emission sources for the period 1980–2020, Atmos. Chem. Phys., 7, 4419-4444, 2007.

Pu, Z., L. Xu, and V. V. Salomonson (2007). MODIS/Terra observed seasonal variations of snow cover over the Tibetan Plateau, *Geophys. Res. Lett.*, 34, L06706, doi:10.1029/2007GL029262.

Qian, Y., Flanner, M. G., Leung, L. R., and Wang, W. 2011: Sensitivity studies on the impacts of Tibetan Plateau snowpack pollution on the Asian hydrological cycle and monsoon climate, Atmos. Chem. Phys., 11, 1929-1948, doi:10.5194/acp-11-1929-2011.

Ramanathan, V., P. J. Crutzen, J. T. Kiehl, and D. Rosenfeld (2001), Aerosols, climate, and the hydrological cycle, Science, 294(5549), 2119–2124.

Ramanathan, V. and G. Carmichael (2008). Global and regional climate changes due to black carbon. *Nature Geoscience*, 1, 221-227.

Rotstayn LD, *et al.* (2012) Aerosol- and greenhouse gas-induced changes in summer rainfall and circulation in the Australasian region: A study using single-forcing climate simulations. Atmos Chem Phys 12:6377–6404.

Taylor, K. E., R. J. Stouffer, and G. A. Meehl (2009), A summary of the CMIP5 experimental design, report, World Clim. Res. Program, Geneva, Switzerland. [Available at http://cmip-pcmdi.llnl.gov/cmip5/experiment_design.html.]

Tobin, D. C., H. E. Revercomb, R. O. Knuteson, B. M. Lesht, L. L. Strow, S. E. Hannon, W. F. Feltz, L. A. Moy, E. J. Fetzer, and T. S. Cress (2006). Atmospheric Radiation Measurement site atmospheric state best estimates for Atmospheric Infrared Sounder temperature and water vapor retrieval validation, J. Geophys. Res., 111, D09S14, doi:10.1029/2005JD006103.

Qian, Y., M. G. Flanner, L. R. Leung, and W. Wang, (2011): Sensitivity studies on the impacts of Tibetan Plateau snowpack pollution on the Asian hydrological cycle and monsoon climate, Atmos. Chem. Phys., 11, 1929-1948, doi:10.5194/acp-11-1929-2011.

APCC TECHNICAL REPORT 2012-02

- Evaluation of Water Balance on a Regional Scale
- Analysis of Climatic Trends over South Asia
- Study of Aerosol Effect on Accelerated Snow Melting
- Aerosol Variability on Global and Regional Scales
- Evaluation of a Distributed Hydrologic Model

APEC Climate Center

12, Centum 7-ro, Haeundae-gu, Busan 612-020,
Republic of Korea
Tel: +82-51-745-3900 Fax: +82-51-745-3949
www.apcc21.org

비매품
9 788997 333370
ISBN 978-89-97333-37-0
ISBN 978-89-97333-35-6 (세트)